Hard Constraints in Optimization Under Uncertainty

Luis G. Crespo*

National Institute of Aerospace

Daniel P. Giesy and Sean P. Kenny†

Dynamic Systems and Control Branch, NASA Langley Research Center

This paper proposes a methodology for the analysis and design of systems subject to parametric uncertainty where design requirements are specified via hard inequality constraints. Hard constraints are those that must be satisfied for all parameter realizations within a given uncertainty model. Uncertainty models given by norm-bounded perturbations from a nominal parameter value, i.e., hyper-spheres, and by sets of independently bounded uncertain variables, i.e., hyper-rectangles, are the focus of this paper. These models, which are also quite practical, allow for a rigorous mathematical treatment within the proposed framework. Hard constraint feasibility is determined by sizing the largest uncertainty set for which the design requirements are satisfied. Analytically verifiable assessments of robustness are attained by comparing this set with the actual uncertainty model. Strategies that enable the comparison of the robustness characteristics of competing design alternatives, the description and approximation of the robust design space, and the systematic search for designs with improved robustness are also proposed. Since the problem formulation is generic and the tools derived only require standard optimization algorithms for their implementation, this methodology is applicable to a broad range of engineering problems.

Keywords: uncertainty, robustness, safety margin, optimization.

I.   Introduction

Design under uncertainty arises in numerous disciplines including engineering, economics, finance and management. Achieving balance between robustness and performance is one of

---

American Institute of Aeronautics and Astronautics

the fundamental challenges faced by scientists and engineers. Trade-offs must be made to reach acceptable levels of performance with adequate robustness to uncertainty.

Literature in stochastic programming[1] and stochastic approximations[2] with applications to structural safety[3,4] and probabilistic controls,[5] provides several mathematical tools for optimization under uncertainty. The algorithms at our disposal can be classified according to the way they enforce inequality constraints that depend on the uncertain parameters. *Hard Constraints*[6–10] are those that, for a given uncertainty model, must be satisfied for all possible realizations of the uncertain parameter (a *realization* is any possible parameter value within the uncertainty model). Strategies to solve the resulting semi-infinite optimization problem usually require nested searches where approximations to the worst-parameter-realization[6,11] are made in a inner optimization loop and a growing number of constraints, which depend on this approximation, are sequentially added to the outer loop. These strategies however, not only become computationally intractable for uncertain parameters of large dimension; but more importantly, are unable to provide guarantees of constraint satisfaction. On the other hand, *Soft Constraints* are those that can be violated by some parameter realizations. Chance-constrained programming,[1] sampling-based techniques,[12–14] asymptotic approximations[5,15] and penalty-based optimization[1,10] are some of the strategies commonly used to handle soft constraints.

For high risk decisions, the achievement and verification of strict constraint feasibility are crucial tasks. This paper addresses these needs by developing a methodology for robustness analysis and robust-design based on the calculation of certain indicators, called Critical Parameter Values and Parametric Safety Margins (PSMs). The ideas proposed do not require sampling/partitioning the parameter space. Instead, they are based on the numerical solution to an optimization problem. Hence, the resulting assessments are as verifiable as the convergence to the global minimum. The reference by Crespo et al.[16] supports the developments to be presented herein.

This paper is organized as follows. An overview of the content is introduced first. This is followed by the motivation and introduction of the mathematical framework. Tests of robustness and extensions to robust design follow. Two simple examples are used to illustrate the scope of the methods proposed. A few concluding remarks close the paper.

II.   Overview

The concern in this paper is the robustness analysis and robust-design of a system described by a parametric mathematical model. The parameters which specify the system are grouped into two categories: uncertain parameters, which are denoted by the vector $\boldsymbol{p}$, and design parameters, which are denoted by the vector $\boldsymbol{d}$.

American Institute of Aeronautics and Astronautics

The uncertainty model of $\boldsymbol{p}$ is composed of a support set $\Delta_{\boldsymbol{p}}$, and a designated point $\bar{p} \in \Delta_{\boldsymbol{p}}$ which will be used as an anchor point for defining expansions and contractions of the support set. The value of the uncertain parameter $\boldsymbol{p}$ is not specified but is assumed to belong to $\Delta_{\boldsymbol{p}}$. In practical applications, the choice of $\Delta_{\boldsymbol{p}}$ is usually made by a discipline expert. However, the theory presented herein acknowledges that such a choice may be fairly arbitrary, and addresses the need for quantifying the level of tolerance of the system to uncertainty in $\boldsymbol{p}$ when a particular $\boldsymbol{d}$ is chosen.

For analysis purposes $\boldsymbol{d}$ is assumed to take on a fixed value, while for design purposes, $\boldsymbol{d}$ is to be chosen. The design requirements for the system are prescribed by a collection of constraint functions, which in general depend on both the uncertain and design parameters. The system is deemed acceptable if all constraint functions are satisfied. For each value of the design parameter, these constraint functions partition the uncertain parameter space into two regions, a failure region, where at least one of the design requirements is not satisfied, and its complement, a safe region where all requirements are satisfied.

One of the tasks of interest is to assign a measure of robustness to a design point based on measuring how much the uncertainty support set can be expanded without encroaching on the failure region. This requires specifying what we mean by expanding the support set. This is where the designated point enters in. Expansion by a factor of α can be viewed in the following way. Imagine standing at the designated point and looking at any other point of the support set. Denote the distance from the designated point to the other point by δ. A *Homothetic* expansion[16] is attained by looking in the same direction and placing the point at a distance of $\alpha\delta$ from the designated point. Note that if α is chosen less than 1, a contraction of the support set is accomplished. In this paper, dilations must be interpreted as homothetic expansions or contractions. For hyper-spherical and hyper-rectangular support sets, we cast the problem of finding the maximal expansion of the support set in terms of an optimization problem to which standard nonlinear constrained optimization algorithms are applicable. The robustness of the corresponding design point is proportional to the size of the maximal expansion.

The failure domain changes with the design point. For each different design point, a measure of robustness can be calculated. One can then search for a design that admits the largest expansion of the support set. We show how to cast this search in the form of a nonlinear optimization problem. The mathematical groundwork for implementing these ideas is presented next.

American Institute of Aeronautics and Astronautics

III.   Framework

The *Uncertainty Model* of the uncertain parameter vector $\boldsymbol{p}$ is given by the *Support Set* $\Delta_{\boldsymbol{p}} \subset \mathbb{R}^{\dim(\boldsymbol{p})}$ and the *Designated Point* $\bar{\boldsymbol{p}} \in \Delta_{\boldsymbol{p}}$ which will be used as an anchor for defining dilations (expansions and contractions) of the support set. The uncertainty model is specified by the analyst/designer. The intent is that the set $\Delta_{\boldsymbol{p}}$ be chosen so that the actual value of the uncertain parameter $\boldsymbol{p}$ lies somewhere within it. A *Realization* of the uncertain parameter is any value of the parameter selected from $\Delta_{\boldsymbol{p}}$. The designated point is the nominal parameter value. Throughout this paper the designated point is chosen to be the geometric center of the support set.

Consider now the situation that a system depends on an uncertain parameter $\boldsymbol{p}$ and a design variable $\boldsymbol{d} \in \mathbb{R}^{\dim(\boldsymbol{d})}$. Suppose that $\boldsymbol{g} : \mathbb{R}^{\dim(\boldsymbol{p})} \times \mathbb{R}^{\dim(\boldsymbol{d})} \to \mathbb{R}^{\dim(\boldsymbol{g})}$ is a set of constraint functions on the system, which have been normalized so that positive values represent constraint violations. If these are considered hard constraints, the system corresponding to given values of $\boldsymbol{d}$ and $\Delta_{\boldsymbol{p}}$ will be judged acceptable if, $\boldsymbol{g}(\boldsymbol{p}, \boldsymbol{d}) \leq \boldsymbol{0}$, $\forall \boldsymbol{p} \in \Delta_{\boldsymbol{p}}$. The *Failure Region*, denoted as $\mathcal{F}(\boldsymbol{d}, \boldsymbol{g}) \subset \mathbb{R}^{\dim(\boldsymbol{p})}$, is composed of the parameters that do not satisfy all the constraints. Specifically, the failure region for the design point $\boldsymbol{d}$ is given by

$$\mathcal{F}(\boldsymbol{d}, \boldsymbol{g}) = \bigcup_{i=1}^{\dim(\boldsymbol{g})} \mathcal{F}_i(\boldsymbol{d}, \boldsymbol{g}),$$

where, for $1 \leq i \leq \dim(\boldsymbol{g})$,

$$\mathcal{F}_i(\boldsymbol{d}, \boldsymbol{g}) = \left\{ \boldsymbol{p} \in \mathbb{R}^{\dim(\boldsymbol{p})} : \boldsymbol{g}_i(\boldsymbol{p}, \boldsymbol{d}) > 0 \right\}.$$

The design $\boldsymbol{d}$ is *Robust* if $\mathcal{F}(\boldsymbol{d}, \boldsymbol{g})$ and $\Delta_{\boldsymbol{p}}$ do not overlap. Otherwise, $\boldsymbol{d}$ is *Non-Robust*. In the former case, the degree of robustness can be quantified by measuring the separation between the two sets.

Selecting the set $\Delta_{\boldsymbol{p}}$ usually involves some engineering judgment. A natural choice for the designated point $\bar{\boldsymbol{p}}$ is the geometric center of $\Delta_{\boldsymbol{p}}$. One reasonable choice for the support set is a hyper-sphere. The hyper-sphere of radius R centered at $\bar{\boldsymbol{p}}$, denoted as $\mathcal{S}_{\boldsymbol{p}}(\bar{\boldsymbol{p}}, R)$, is defined by

$$\mathcal{S}_{\boldsymbol{p}}(\bar{\boldsymbol{p}}, R) = \left\{ \boldsymbol{p} : \|\bar{\boldsymbol{p}} - \boldsymbol{p}\| \leq R \right\}.$$

Another reasonable choice might be to confine each component of $\boldsymbol{p}$ to a bounded interval. This is especially desirable when the levels of uncertainty in $\boldsymbol{p}$ are dissimilar. This leads to the choice of $\Delta_{\boldsymbol{p}}$ as a hyper-rectangle. If $\boldsymbol{m}$ is the vector of half-lengths of the sides of the

American Institute of Aeronautics and Astronautics

rectangle, the hyper-rectangle $\mathcal{R}_{\boldsymbol{p}}(\bar{\boldsymbol{p}}, \boldsymbol{m})$ is defined by

$$\mathcal{R}_{\boldsymbol{p}}(\bar{\boldsymbol{p}}, \boldsymbol{m}) = \{\boldsymbol{p} : \boldsymbol{p}_i \in [\bar{\boldsymbol{p}}_i - \boldsymbol{m}_i, \bar{\boldsymbol{p}}_i + \boldsymbol{m}_i], 1 \leq i \leq \dim(\boldsymbol{p})\}.$$

For purposes of this paper, two uncertainty models will be called *Proportional* if they have the same designated point and they are homothetic with respect to that designated point. Therefore, one of the two support sets can be formed from the other by expansion or contraction by some positive factor about the common designated point. Call such a factor the *Similitude Ratio* and denote it by α. For instance, the hyper-rectangles $\mathcal{R}_{\boldsymbol{p}}(\bar{\boldsymbol{p}}, \boldsymbol{m})$ and $\mathcal{R}_{\boldsymbol{p}}(\bar{\boldsymbol{p}}, \alpha \boldsymbol{m})$ are proportional sets. The relationship between two proportional models, say A and B, will be denoted as $A = \mathcal{H}(B, \bar{\boldsymbol{p}}, \alpha)$.

The notions of Critical Parameter Value and PSM are now introduced. For clarity sake, the presentation of the material will concentrate on the case where the designated point is in the non-failure region. The converse case is considered in Section IV-D. Intuitively, one imagines that a set proportional to the support set of the uncertainty model is being expanded homotheticly with respect to its designated point until its boundary just touches the boundary of the failure region. The point(s) where the expanding set touches the failure region is (are) the Critical Parameter Value(s). The *Critical Similitude Ratio* is the similitude ratio of that expansion, and the PSM is a metric that quantifies the size of the set proportional to the support set that has the Critical Parameter Value on its surface. Both the Critical Similitude Ratio, which is defined for all support sets, and the PSM, which is defined for support sets which are hyper-spheres or hyper-rectangles, provide a measure of robustness of a design to parameter uncertainty. The larger they are, the larger the variation from its designated point to which the uncertain parameter can be subjected without encountering a constraint violation. The Critical Similitude Ratio is non-dimensional, but depends on both the shape and the size of the support set. The PSM has the same units as the uncertain parameters, and depends on the shape, but not the size, of the support set. The mathematical background for these notions is presented next.

Denote by ∂ the set boundary operator. Let $\boldsymbol{d}$ be a given design and let $\Delta_{\boldsymbol{p}}$, $\bar{\boldsymbol{p}}$, and $\boldsymbol{g}$ be prescribed in advance. Any $\tilde{\boldsymbol{p}}$ lying in $\partial \mathcal{H}(\Delta_{\boldsymbol{p}}, \bar{\boldsymbol{p}}, \tilde{\alpha}) \cap \partial \mathcal{F}$ will be the *Critical Parameter Value* for this design, uncertainty model, and constraint set. Note that the Critical Parameter Value might not be a realization of the uncertain parameter; i.e., $\tilde{\boldsymbol{p}}$ might not belong to $\Delta_{\boldsymbol{p}}$. Further note that the Critical Parameter Value might not be uniquely determined; i.e., $\partial \mathcal{H}(\Delta_{\boldsymbol{p}}, \bar{\boldsymbol{p}}, \tilde{\alpha}) \cap \partial \mathcal{F}$ might contain several points. Figures 1 and 2 show sketches with relevant metrics for hyper-spherical and hyper-rectangular supports respectively.

A design point is deemed to be in the *Feasible Design Space* if it satisfies all the constraints when the uncertain parameter assumes the value of the designated point. The *Robust Design*

Space is the set of designs satisfying the hard constraints for all points of the uncertainty set of a given uncertainty model. Each member of the Robust Design Space set is a robust design. Note that if the Robust Design Space exists, it is a subset of the Feasible Design Space. Formal definitions of the PSMs for hyper-spherical and hyper-rectangular supports are provided in Section IV, as are expressions for the calculation of these PSMs. In general, the PSM is uniquely specified by the design point $\boldsymbol{d}$, the support set $\Delta_{\boldsymbol{p}}$, the designated point $\bar{\boldsymbol{p}}$, the constraint functions $\boldsymbol{g}$, and the similitude ratio $\tilde{\alpha}$. The PSM is proportional to the degree of robustness of $\boldsymbol{d}$ to uncertainty in $\boldsymbol{p}$. If the PSM assumes the value of zero, there is no robustness since at least one of the constraints is active for $\bar{\boldsymbol{p}}$, i.e. since $\bar{\boldsymbol{p}}$ is on the boundary of the failure region there exist arbitrarily small perturbations from $\bar{\boldsymbol{p}}$ leading to a constraint violation. The convention is that designs within the Feasible Design Space assume non-negative PSM values, otherwise they are negative.

IV. Robustness Analysis

Problem Statement: Does the design $\boldsymbol{d}$ satisfy the hard constraints $\boldsymbol{g}(\boldsymbol{p}, \boldsymbol{d}) \leq \boldsymbol{0}$ for each $\boldsymbol{p} \in \Delta_{\boldsymbol{p}}$?

When the structure of the support set is restricted, robustness tests can be established. A general test applicable to compact sets is available[16] in the literature. Robustness tests for hyper-spherical and hyper-rectangular support sets are considered next. These strategies are then used to handle supports with other geometries. In what follows we assume that $\boldsymbol{g}(\bar{\boldsymbol{p}}, \boldsymbol{d}) < \boldsymbol{0}$ and $\partial \mathcal{F}_j = \{\boldsymbol{p} : \boldsymbol{g}_j(\boldsymbol{p}, \boldsymbol{d}) = 0\}$ for $1 \leq j \leq \dim(\boldsymbol{g})$.

A. Hyper-Spheres

Hyper-spherical support sets result from uncertainty models where uncertainty is described by norm bounded perturbations from the nominal parameter value $\bar{\boldsymbol{p}}$. This implies that $\Delta_{\boldsymbol{p}}$ is a hyper-sphere and $\bar{\boldsymbol{p}}$ is its geometric center. Problems with this class of support sets are the simplest since the Critical Parameter Value is calculated by solving a set of minimum norm problems in $\boldsymbol{p}$-space. The Critical Parameter Value, denoted hereafter as $\tilde{\boldsymbol{p}}$, for $\Delta_{\boldsymbol{p}} = \mathcal{S}_{\boldsymbol{p}}(\bar{\boldsymbol{p}}, R)$ is the $\boldsymbol{p}$ value on the surface of the failure region that minimizes $\|\boldsymbol{p} - \bar{\boldsymbol{p}}\|$, i.e.,

$$\tilde{\boldsymbol{p}} = \operatorname*{argmin}_{\boldsymbol{p}} \{\|\boldsymbol{p} - \bar{\boldsymbol{p}}\| : \boldsymbol{p} \in \partial \mathcal{F}\}. \tag{1}$$

This optimization problem is restated as

$$\tilde{\boldsymbol{p}} = \tilde{\boldsymbol{p}}^{(i)}, \tag{2}$$

where

$$i = \operatorname*{argmin}_{1 \leq j \leq \dim(\boldsymbol{g})} \left\{ \|\tilde{\boldsymbol{p}}^{(j)} - \bar{\boldsymbol{p}}\| \right\}, \tag{3}$$

and

$$\tilde{\boldsymbol{p}}^{(j)} = \operatorname*{argmin}_{\boldsymbol{p}} \left\{ \|\boldsymbol{p} - \bar{\boldsymbol{p}}\| : \boldsymbol{g}_j(\boldsymbol{p}, \boldsymbol{d}) = 0 \right\}. \tag{4}$$

Hence, the Critical Parameter Value problem is solved for each individual constraint function, and the answer is selected which is closest to the designated point. Note that the equality constraint in Equation (4) is a particular case of $\boldsymbol{p} \in \partial \mathcal{F}_j$. By applying certain properties[16] in this equation, the constraint $\boldsymbol{g}_j = 0$ can be replaced by $\boldsymbol{g}_j \geq 0$.

The *Spherical PSM* corresponding to the design $\boldsymbol{d}$ for $\Delta_{\boldsymbol{p}} = \mathcal{S}_{\boldsymbol{p}}(\bar{\boldsymbol{p}}, R)$ is defined as

$$\rho_{\mathcal{S}}(\bar{\boldsymbol{p}}, \tilde{\boldsymbol{p}}, \boldsymbol{d}) \overset{\Delta}{=} \|\tilde{\boldsymbol{p}} - \bar{\boldsymbol{p}}\|, \tag{5}$$

where $\bar{\boldsymbol{p}}$ is the designated point of the uncertainty model and $\tilde{\boldsymbol{p}}$ is a corresponding Critical Parameter Value. If $\tilde{\alpha}$ is the similitude ratio corresponding to the set containing the Critical Parameter Value on its surface, $\rho_{\mathcal{S}} = \tilde{\alpha} R$.

A simple robustness test for hyper-spherical supports sets can now be formulated.

P-Test: The design $\boldsymbol{d}$ satisfies the hard constraints prescribed by $\Delta_{\boldsymbol{p}} = \mathcal{S}_{\boldsymbol{p}}(\bar{\boldsymbol{p}}, R)$ and $\boldsymbol{g}(\boldsymbol{p}, \boldsymbol{d}) \leq \boldsymbol{0}$ if and only if $\rho_{\mathcal{S}} \geq R$. This condition is equivalent to $\tilde{\alpha} \geq 1$.

A sketch showing relevant quantities is displayed in Figure 1. The Robust Design Space corresponding to $\Delta_{\boldsymbol{p}} = \mathcal{S}_{\boldsymbol{p}}(\bar{\boldsymbol{p}}, R)$ is given by $\{\boldsymbol{d} : \rho_{\mathcal{S}} \geq R\}$, whose boundary is the iso-spherical-PSM manifold $\rho_{\mathcal{S}} = R$.

B. Hyper-Rectangles

When each component of the uncertain parameter is confined to a prescribed interval, the support set is a hyper-rectangle. Note that this geometry allows for the manipulation of sets of parameters having different units and levels of uncertainty. Recall that if $\bar{\boldsymbol{p}}$ is the geometric center of the hyper-rectangle, and $\boldsymbol{m}$ is the vector of half-lengths of its sides, the resulting hyper-rectangle is denoted as $\mathcal{R}_{\boldsymbol{p}}(\bar{\boldsymbol{p}}, \boldsymbol{m})$. A robustness test for supports with this geometry is introduced in this section. The mathematical background for this is presented next.
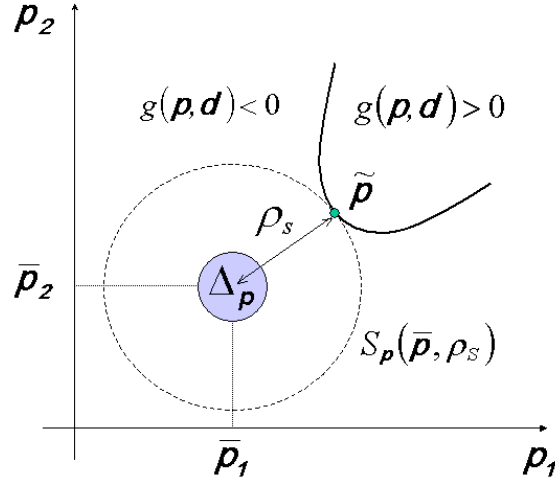
Figure 1. Relevant metrics for a circular support.

1. Q-transformation

Let $\Delta_{\boldsymbol{p}} = \mathcal{R}_{\boldsymbol{p}}(\bar{\boldsymbol{p}}, \boldsymbol{m})$ be the support of $\boldsymbol{p}$. The *Q-Transformation*, denoted as $\boldsymbol{q} = Q(\boldsymbol{p})$, is given by

$$\boldsymbol{q} \triangleq \frac{\max\{|\boldsymbol{k}|\}\boldsymbol{k}}{\|\boldsymbol{k}\|} \tag{6}$$

where

$$\boldsymbol{k} = \mathrm{diag}\{\boldsymbol{m}\}^{-1}\,(\boldsymbol{p} - \bar{\boldsymbol{p}})\,. \tag{7}$$

The corresponding inverse transformation, $\boldsymbol{p} = Q^{-1}(\boldsymbol{q})$, is given by

$$\boldsymbol{p} = \bar{\boldsymbol{p}} + \frac{\|\boldsymbol{q}\|\mathrm{diag}\{\boldsymbol{m}\}\boldsymbol{q}}{\max\{|\boldsymbol{q}|\}}\,. \tag{8}$$

The Q-Transformation transforms $\mathcal{R}_{\boldsymbol{p}}(\bar{\boldsymbol{p}}, \boldsymbol{m})$ into a unit hyper-sphere in $\boldsymbol{q}$-space centered at the origin. Q maps sets proportional to the hyper-rectangle to sets proportional to the hyper-sphere while preserving the similitude ratio, i.e.,

$$Q(\mathcal{H}(\mathcal{R}_{\boldsymbol{p}}(\bar{\boldsymbol{p}}, \boldsymbol{m}), \bar{\boldsymbol{p}}, \alpha)) = \mathcal{H}(\mathcal{S}_{\boldsymbol{q}}(\boldsymbol{0}, 1), \boldsymbol{0}, \alpha) = \mathcal{S}_{\boldsymbol{q}}(\boldsymbol{0}, \alpha).$$

Notice that the Q-transformation introduces derivative discontinuities. These discontinuities occur at points corresponding to $\boldsymbol{p}$-space points where the faces of hyper-rectangles proportional to the support set meet.

The Q-transformation enables the easy manipulation of hyper-rectangular sets, e.g., sampling their volumes, surfaces, and determining if a given $\boldsymbol{p}$ is within the set. More importantly, it allows the identification of the corresponding Critical Parameter Value by solving

American Institute of Aeronautics and Astronautics

a set of minimum norm problems in $\boldsymbol{q}$-space. Specifically, the Critical Parameter Value can be found by solving

$$\tilde{\boldsymbol{p}} = \tilde{\boldsymbol{p}}^{(i)}, \tag{9}$$

where

$$i = \operatorname*{argmin}_{1 \leq j \leq \dim(\boldsymbol{g})} \left\{ \|Q(\tilde{\boldsymbol{p}}^{(j)})\| \right\}, \tag{10}$$

and

$$\tilde{\boldsymbol{p}}^{(j)} = \operatorname*{argmin}_{\boldsymbol{p}} \left\{ \|Q(\boldsymbol{p})\| : \boldsymbol{g}_j\left(\boldsymbol{p}, \boldsymbol{d}\right) = 0 \right\}. \tag{11}$$

Hence, the Critical Parameter Value problem is solved for each individual constraint function, and the answer is the one whose norm in $\boldsymbol{q}$-space is the smallest. As before, properties of the Critical Parameter Value allows us to replace the equality constraint with an inequality constraint.

The *Rectangular PSM* corresponding to the design $\boldsymbol{d}$ for $\Delta_{\boldsymbol{p}} = \mathcal{R}_{\boldsymbol{p}}(\bar{\boldsymbol{p}}, \boldsymbol{m})$, is defined as

$$\rho_{\mathcal{R}}\left(\bar{\boldsymbol{p}}, \tilde{\boldsymbol{p}}, \boldsymbol{m}, \boldsymbol{d}\right) \triangleq \left\| Q^{-1}\left(\frac{\|Q(\tilde{\boldsymbol{p}})\| \cdot \mathbf{1}}{\sqrt{\dim(\boldsymbol{p})}} \right) - \bar{\boldsymbol{p}} \right\|, \tag{12}$$

which is equivalent to $\tilde{\alpha}\|\boldsymbol{m}\|$.

A sketch showing relevant quantities is displayed in Figure 2. Note that $\hat{\boldsymbol{p}} = \bar{\boldsymbol{p}} + \tilde{\alpha}\boldsymbol{m}$ and $\hat{\boldsymbol{q}} = Q(\hat{\boldsymbol{p}})$. As always, $\mathcal{H}(\mathcal{R}, \bar{\boldsymbol{p}}, \tilde{\alpha})$ is the maximum set proportional to the support set of the
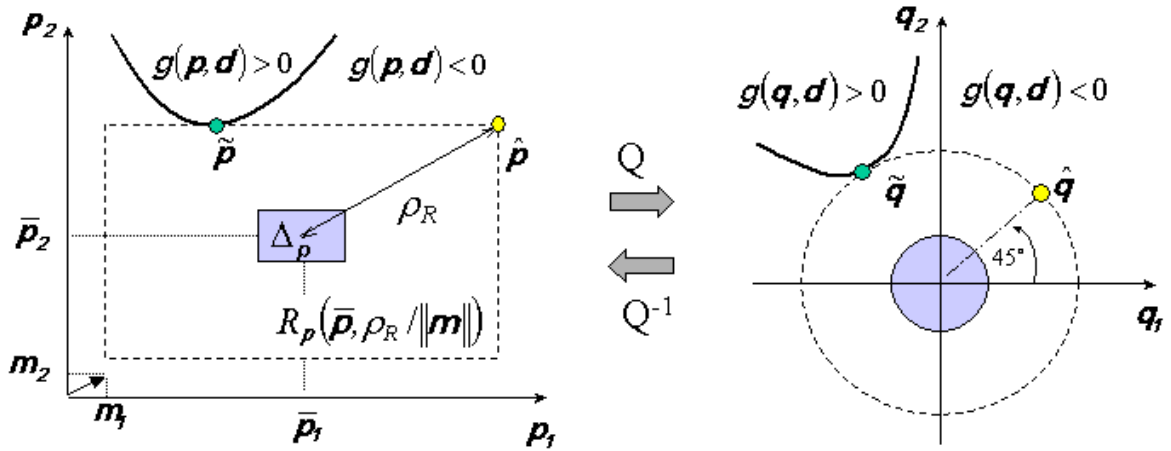

Figure 2. Relevant metrics for a rectangular support.

uncertainty model which contains no constraint violation points. The rectangular-PSM is related to the diagonal measure of this hyper-rectangle. This provides comparability between rectangular-PSMs measured, for example, for different design points and therefore different constraint geometries and different locations of the Critical Parameter Value. Note that

$\mathcal{H}(\mathcal{R}, \bar{\boldsymbol{p}}, \tilde{\alpha})$ is inscribed in a hyper-sphere centered at $\bar{\boldsymbol{p}}$ of radius equal to its rectangular-PSM.

2. Infinity Norm Formulation

An alternative way to search for the Critical Parameter Value for hyper-rectangular supports is presented here. This formulation allows us to circumvent the problems caused by discontinuities in the gradient of the Q-Transformation.

Recall that the infinity norm in a finite dimensional space is defined as $\|\boldsymbol{x}\|^{\infty} = \sup_i\{|\boldsymbol{x}_i|\}$. Let us define the $\boldsymbol{m}$-scaled infinity norm as $\|\boldsymbol{x}\|_{\boldsymbol{m}}^{\infty} = \sup_i\{|\boldsymbol{x}_i|/\boldsymbol{m}_i\}$. A distance between the vectors $\boldsymbol{x}$ and $\boldsymbol{y}$ can be defined as $\|\boldsymbol{x} - \boldsymbol{y}\|_{\boldsymbol{m}}^{\infty}$. Using this distance, the unit ball centered at $\bar{\boldsymbol{p}}$ is just $\mathcal{R}(\bar{\boldsymbol{p}}, \boldsymbol{m})$.

In this context, for a given $\boldsymbol{d}$, the Critical Parameter Value for the vector of constraint functions $\boldsymbol{g}(\boldsymbol{p}, \boldsymbol{d})$ and for an uncertainty model with support set $\mathcal{R}(\bar{\boldsymbol{p}}, \boldsymbol{m})$ and designated point $\bar{\boldsymbol{p}}$, results from using the $\boldsymbol{m}$-scaled infinity norm in Equation (1). This optimization problem is restated as

$$\tilde{\boldsymbol{p}} = \tilde{\boldsymbol{p}}^{(i)}, \tag{13}$$

where

$$i = \operatorname*{argmin}_{1 \leq j \leq \dim(\boldsymbol{g})} \left\{ \|\tilde{\boldsymbol{p}}^{(j)} - \bar{\boldsymbol{p}}\|_{\boldsymbol{m}}^{\infty} \right\}, \tag{14}$$

and

$$\tilde{\boldsymbol{p}}^{(j)} = \operatorname*{argmin}_{\boldsymbol{p}}\{\|\boldsymbol{p} - \bar{\boldsymbol{p}}\|_{\boldsymbol{m}}^{\infty} : \boldsymbol{g}_j(\boldsymbol{p}, \boldsymbol{d}) = 0\}. \tag{15}$$

Hence, the Critical Parameter Value problem is solved for each individual constraint function, and the answer is selected which is closest to the designated point in the $\boldsymbol{m}$-scaled infinity norm. The reader should realize the similarities among the sets of Equations (2-4), (9-11), and (13-15). Rewriting this using the definition of the $\boldsymbol{m}$-scaled infinity norm gives

$$\tilde{\boldsymbol{p}}^{(j)} = \operatorname*{argmin}_{\boldsymbol{p}} \left\{ \max_{1 \leq k \leq \dim(\boldsymbol{p})} \frac{|\boldsymbol{p}_k - \bar{\boldsymbol{p}}_k|}{\boldsymbol{m}_k} : \boldsymbol{g}_j(\boldsymbol{p}, \boldsymbol{d}) = 0 \right\}.$$

The "max" can be eliminated and the objective function made differentiable by introducing the similitude ratio α defined earlier

$$\langle \tilde{\boldsymbol{p}}^{(j)}, \tilde{\alpha}^{(j)} \rangle = \operatorname*{argmin}_{\boldsymbol{p}, \alpha}\{\alpha : \boldsymbol{g}_j(\boldsymbol{p}, \boldsymbol{d}) = 0, |\boldsymbol{p}_k - \bar{\boldsymbol{p}}_k| \leq \alpha \boldsymbol{m}_k, 1 \leq k \leq \dim(\boldsymbol{p})\}. \tag{16}$$

This eliminates non-differentiabilities in the objective functions. Assuming that the constraint functions $\boldsymbol{g}$ are continuous, the problem at hand is turned into an "inequality constraint only" optimization problem, which is more "optimizer friendly", by changing the

constraint on g_j from $g_j = 0$ to $g_j \geq 0$ since the optimum must occur on $\partial \mathcal{F}$. For a fixed d, if i is given by Equation (14) and $\tilde{\alpha} = \tilde{\alpha}^{(i)}$, $\tilde{p} = \tilde{p}^{(i)}$ is the Critical Parameter Value and $\mathcal{R}_p(\bar{p}, \tilde{\alpha}m)$ is the largest hyper-rectangle proportional to $\mathcal{R}_p(\bar{p}, m)$ which fits inside the non-failure region of the p-space. Another interpretation is that $\tilde{\alpha}$ is the radius of the largest unit sphere (in the m-scaled infinity norm metric) centered at $\bar{p}$ which fits inside the p-space feasible set for the given design d.

With these concepts at hand, a robustness test for hyper-rectangular support sets is formulated as follows

Q-Test: The design d satisfies the hard constraints prescribed by $\Delta_p = \mathcal{R}_p(\bar{p}, m)$ and $g(p, d) \leq 0$ if and only if $\|Q(\tilde{p})\| \geq 1$. This condition is equivalent to $\|\tilde{p} - \bar{p}\|_m^\infty \geq 1$, and to $\rho_\mathcal{R} \geq \|m\|$.

Recall that the Critical Parameter Values are p values, not necessarily realizations of p, at the verge of violating at least one of the constraints. The Robust Design Space corresponding to $\Delta_p = \mathcal{R}_p(\bar{p}, m)$ is given by $\{d : \rho_\mathcal{R} \geq \|m\|\}$, whose boundary is the iso-rectangular-PSM manifold $\rho_\mathcal{R} = \|m\|$.

C.   Bounding Sets

We next look at how the techniques developed so far can be leveraged to provide robustness tests for support sets with other geometries. The tests and margins above enable a rigorous assessment of hyper-spherical and hyper-rectangular sets. In this section we use these geometries as bounding sets of support sets having arbitrary shapes. Studies on the bounding sets will be used to infer properties of the support set. Conservatism is unavoidably introduced since the design requirements apply to the actual support set, not to the bounding set.

Bounding Test: Let the support set Δ_p be of arbitrary shape. Define an outer bounding set $\mathcal{O}_p$ as one satisfying $\Delta_p \subseteq \mathcal{O}_p$. If the design d satisfies the hard constraints for the bounding set $\mathcal{O}_p$, the design d satisfies the hard constraints for Δ_p; i.e., the design is robust. On the other hand, if the design d does not satisfy the hard constraints for as much as one realization $p \in \Delta_p$, the design d does not satisfy the hard constraints for Δ_p; i.e., the design is not robust.

The P- and the Q-tests can be used to determine the robustness of hyper-spherical and hyper-rectangular bounding sets. Obviously, conservatism is reduced by using tighter bounding sets. Constraint violations caused by parameter values in the intersection between $\mathcal{O}_p$ and the complement set of Δ_p might cause a robust design to fail the Bounding Test. Con-

servative approximations to the Robust Design Space for arbitrarily shaped support sets can be easily calculated using PSMs. For instance, if $\mathcal{O}_{\boldsymbol{p}} = \mathcal{S}_{\boldsymbol{p}}(\bar{\boldsymbol{p}}, R)$, the design set $\{\boldsymbol{d} : \rho_{\mathcal{S}} \geq R\}$ is a subset of the actual Robust Design Space.

D.   Designs outside the Feasible Design Space

Thus far we have only considered the case in which the designated point is in the Feasible Design Space. An extension to the converse case, for which $\boldsymbol{g}(\bar{\boldsymbol{p}}, \boldsymbol{d})$ has at least one positive component, is introduced next. One situation in which a need for this extension might arise is if an automated, optimization driven design procedure varies the design parameter so much that constraint boundaries move enough to make $\bar{\boldsymbol{p}}$ a constraint violation point. If $\bar{\boldsymbol{p}} \in \mathcal{F}^c$ (where the super-script c denotes the set complement operator), the Critical Parameter Value for hyper-spherical support sets is given by

$$\begin{aligned}
\tilde{\boldsymbol{p}} &= \underset{\boldsymbol{p}}{\operatorname{argmin}} \left\{ \|\boldsymbol{p} - \bar{\boldsymbol{p}}\| : \boldsymbol{p} \in \mathcal{F}^c \right\}, \\
&= \underset{\boldsymbol{p}}{\operatorname{argmin}} \left\{ \|\boldsymbol{p} - \bar{\boldsymbol{p}}\| : \boldsymbol{g}_i(\boldsymbol{p}, \boldsymbol{d}) \leq 0, \quad i = 1, \cdots, \dim(\boldsymbol{g}) \right\}.
\end{aligned} \tag{17}$$

Expressions for hyper-rectangular support sets are obtained by using $\|Q(\boldsymbol{p})\|$ instead of $\|\boldsymbol{p} - \bar{\boldsymbol{p}}\|$ in Equation (17). The corresponding PSMs result from multiplying the right hand side of Equations (5) and (12) by minus one. Therefore, designs outside the Feasible Design Space will have negative PSMs. Results must be interpreted accordingly.

Numerical methods typically used to handle soft constraints, such as sampling and reliability methods, are unable to properly address the opening problem statement of Section IV. Tools for handling soft constraints are based on the estimation of $P[\mathcal{F}]$, the probability of failure. For hard constraints this probability is zero. Sampling-based methods can wrongly predict zero failure probabilities as a result of the numerical error incurred by using a finite number of samples. On the other hand, methods based on asymptotic approximations such as the First-Order Reliability Method (FORM), will not converge since the limit state surface $\partial \mathcal{F}$ does not exist in standard normal space.

For a given set of design requirements, different design architectures lead to different constraint structures. PSMs allow for the unbiased comparison of the robustness characteristics of competing design alternatives having different design architectures. For instance, if $\boldsymbol{d1}$ is a design alternative within the design architecture $\mathcal{D}1$ leading to the set of constraints $\boldsymbol{g1}$, and $\boldsymbol{d2}$ is another design alternative within the architecture $\mathcal{D}2$ leading to $\boldsymbol{g2}$, a comparison of the robustness of $\boldsymbol{d1}$ and $\boldsymbol{d2}$ can be made even though the way in which $\boldsymbol{g1}$ and $\boldsymbol{g2}$ depend upon $\boldsymbol{p}$ and $\boldsymbol{d}$ is different.

American Institute of Aeronautics and Astronautics

V.   Robust-Design

Problem Statement: For a given support set $\Delta_{\boldsymbol{p}}$ and a given designated point $\bar{\boldsymbol{p}}$, find the design $\boldsymbol{d}^*$ whose PSM is the largest.

This problem can be posed as follows:

$$\boldsymbol{d}^* = \underset{\boldsymbol{d}}{\operatorname{argmax}} \left\{ \tilde{\alpha}(\bar{\boldsymbol{p}}, \Delta_{\boldsymbol{p}}, \boldsymbol{d}, \boldsymbol{g}) \right\}.$$

If $\tilde{\alpha}^*$ is the Critical Similitude Ratio corresponding to $\boldsymbol{d}^*$, the set $\mathcal{M}(\Delta_{\boldsymbol{p}}, \bar{\boldsymbol{p}}, \tilde{\alpha}^*)$, called the *Maximum Feasible Set*, is the largest set proportional to $\Delta_{\boldsymbol{p}}$ for which hard constraints are feasible. Design strategies for hyper-spherical and hyper-rectangular support sets are presented next. The former case will be referred to as the P-Search while the latter one as the Q-Search.

The uniqueness of the solution to the problem statement above cannot be guaranteed unless restrictions[6, 15] on the way in which $\boldsymbol{g}$ depends on $\boldsymbol{p}$ apply. It may be possible to find designs whose Critical Parameter Value does not exist, i.e., designs leading to an unbounded $\mathcal{M}$. In these cases, $\boldsymbol{d}$ is able to eliminate the dependence of the constraints on the uncertain parameter.

P-Search: If $\boldsymbol{g} \leq \boldsymbol{0}$ is a set of constraints and $\mathcal{S}_{\boldsymbol{p}}(\bar{\boldsymbol{p}}, R)$ is the support set, a design with the best robustness characteristics, namely $\boldsymbol{d}^{\mathcal{S}}$, and the corresponding maximum feasible set are given by

$$\boldsymbol{d}^{\mathcal{S}} = \underset{\boldsymbol{d}}{\operatorname{argmin}} \left\{ -\rho_{\mathcal{S}}(\bar{\boldsymbol{p}}, \tilde{\boldsymbol{p}}, \boldsymbol{d}) \right\}, \tag{18}$$

$$\mathcal{M} = \mathcal{S}_{\boldsymbol{p}} \left(\bar{\boldsymbol{p}}, \rho_{\mathcal{S}}(\bar{\boldsymbol{p}}, \tilde{\boldsymbol{p}}, \boldsymbol{d}^{\mathcal{S}}) \right). \tag{19}$$

Q-Search: If $\boldsymbol{g} \leq \boldsymbol{0}$ is a set of constraints and $\mathcal{R}_{\boldsymbol{p}}(\bar{\boldsymbol{p}}, \boldsymbol{m})$ is the support set, a design with the best robustness characteristics, namely $\boldsymbol{d}^{\mathcal{R}}$, and the corresponding maximum feasible set are given by

$$\boldsymbol{d}^{\mathcal{R}} = \underset{\boldsymbol{d}}{\operatorname{argmin}} \left\{ -\rho_{\mathcal{R}}(\bar{\boldsymbol{p}}, \tilde{\boldsymbol{p}}, \boldsymbol{m}, \boldsymbol{d}) \right\}, \tag{20}$$

$$\mathcal{M} = \mathcal{R}_{\boldsymbol{p}} \left(\bar{\boldsymbol{p}}, \frac{\rho_{\mathcal{R}}(\bar{\boldsymbol{p}}, \tilde{\boldsymbol{p}}, \boldsymbol{m}, \boldsymbol{d}^{\mathcal{R}})\boldsymbol{m}}{\|\boldsymbol{m}\|} \right). \tag{21}$$

Note that $-\|\tilde{\boldsymbol{q}}\|$ can also be used as the objective of the optimization problem in Equation (20). Details on the derivation of Equation (21) and on the existence of the Robust Design

American Institute of Aeronautics and Astronautics

Space are available[16] in the literature.

Sizing $\mathcal{M}$ is an important task in reliability-based design optimization. Probabilistic techniques, typically used to handle soft inequality constraints, should not be used when the support set of the probability density function of the uncertain parameter is a subset of $\mathcal{M}$. Otherwise, numerical error might lead to the false identification of robust designs.

VI. Examples

The methods and tools proposed herein are applicable to realistic engineering problems, which are in general multi-dimensional, non-linear and for which explicit expressions for the design requirements are usually unavailable. However, the examples presented next have been chosen in order to enable the visualization and reproducibility of the results.

A. Two-dimensional Example

A two-dimensional problem in the design variables, i.e., $\boldsymbol{d} = [\boldsymbol{d}_1, \boldsymbol{d}_2]^T$, and in the uncertain parameter, i.e., $\boldsymbol{p} = [\boldsymbol{p}_1, \boldsymbol{p}_2]^T$, is considered here. Let the set of constraints be prescribed by

$$
\boldsymbol{g} = \begin{bmatrix} 3\boldsymbol{d}_2 - 4\boldsymbol{p}_1^2 - 4\boldsymbol{d}_1\boldsymbol{p}_2 \sin\left(\boldsymbol{p}_2\boldsymbol{d}_1 - \boldsymbol{p}_1^2\right) \\ -\sin\left(\boldsymbol{p}_1^2\boldsymbol{p}_2 - \sin(2\boldsymbol{p}_1 - 2)\right) - \boldsymbol{d}_1\boldsymbol{d}_2\boldsymbol{p}_1 - \boldsymbol{p}_2 \\ \boldsymbol{d}_1 + \boldsymbol{p}_1^2\boldsymbol{d}_2^2 - 4\boldsymbol{p}_2^2\boldsymbol{p}_1 - 4\sin\left(2\boldsymbol{p}_1 - 2\boldsymbol{p}_2\right) \\ 2(\boldsymbol{p}_1 + \boldsymbol{p}_2)\sin(\boldsymbol{p}_1^2 - \boldsymbol{d}_2) - 2\boldsymbol{p}_1\boldsymbol{p}_2\left(\boldsymbol{d}_2 + 2\boldsymbol{p}_1^2 - 2\right) + \boldsymbol{d}_1 - 6\boldsymbol{p}_1 \end{bmatrix},
$$

and the designated point be $\bar{\boldsymbol{p}} = [1, 1]^T$. The contour of the corresponding Feasible Design Space is marked with a solid thick line in subsequent figures.

This first illustration makes use of a spherical support set, $\Delta_{\boldsymbol{p}}$, centered at $\bar{\boldsymbol{p}}$. This choice of support set might indicate the analyst's judgment that the uncertainty in the uncertain parameter is geometrical in nature with no distinctions made based on the direction of perturbation from the designated point. For different design points in the Feasible Design Space, the PSM $\rho_{\mathcal{S}}$ is calculated. The resulting PSMs are shown as a function of the design point $\boldsymbol{d}$ in Figure 3. Recall that, for a given design point, its PSM is the size of the largest perturbation to $\bar{\boldsymbol{p}}$ allowed before a constraint is violated. For ease of comparability, the color scale used in Figure 3 is the same as that in subsequent figures. This figure illustrates that the design with best robustness characteristics is able to tolerate uncertainty in $\boldsymbol{p} = \bar{\boldsymbol{p}} + \boldsymbol{u}$ with $\|\boldsymbol{u}\| \leq 0.53$. Therefore, variations of less than 0.53 lead to non-empty Robust Design Spaces. The boundary of the Feasible Design Space is given by the $\rho_{\mathcal{S}} = 0$ contour. Notice that multiple PSM maxima occur (there are local maxima in the vicinity of $[-1, 0]^T$ and of $[-2.2, -2.4]^T$). More importantly, notice that designs further in from the boundary of the

Feasible Design Space are not necessarily more robust. This fact is counterintuitive. For instance, the comparison of $d1 = [-2.25, -2.4]^T$ and $d2 = [-1, -1]^T$ shows that $\rho_S(d1) \gg \rho_S(d2)$ even though $d1$ is much closer to a constraint limiting the Feasible Design Space than $d2$. This behavior is contrary to the general perception.
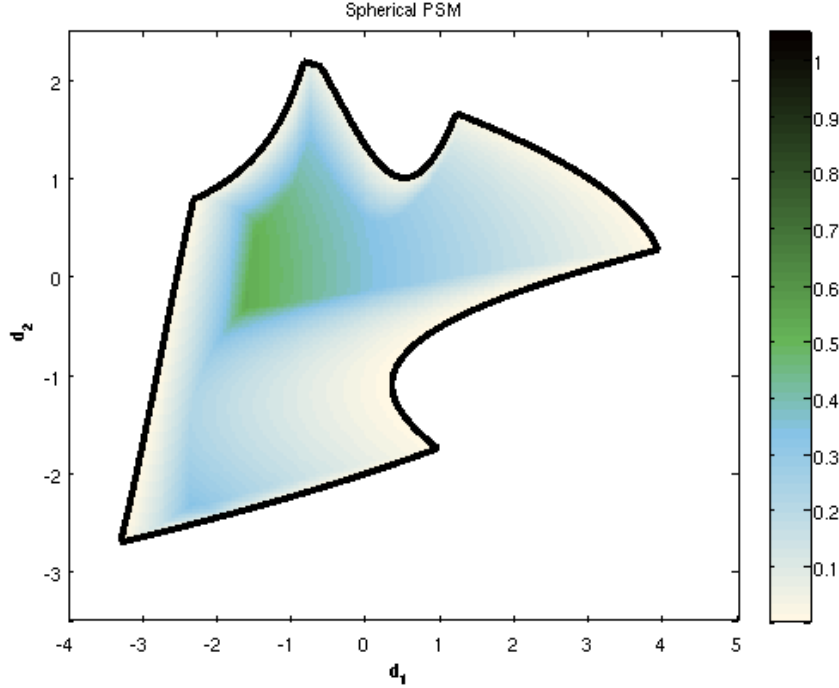

Figure 3. Spherical PSMs.

Now we consider the square support set $\Delta_p = \mathcal{R}_p(\bar{p}, m1)$, where $m1 = [1, 1]^T$. This choice of support set might indicate the analyst's judgment that the uncertainties in the components of the uncertain parameter are independent of each other, but of about the same magnitude. The corresponding rectangular-PSM are shown in Figure 4. Larger margins are now attained. Similarities in the distribution of PSMs arise since the offsets between the circles, i.e., two-dimensional hyper-spheres, and the squares, i.e., two dimensional regular hyper-rectangles, used are relatively small. Figure 5 shows the rectangular-PSM values for $\mathcal{R}_p(\bar{p}, m2)$ where $m2 = [1, 4]^T$. This choice of support set might indicate the analyst's judgment that the uncertainties in the components of the uncertain parameter are independent of each other, and that the level of uncertainty in the second component is about 4 times that of the first. Considerable differences in the distribution and magnitude of the PSMs, as compared to the previous two figures, are apparent. This indicates a strong dependence of the robustness on the geometry of the support set.

An application of the material of Section IV-C on bounding sets is now presented. Con-
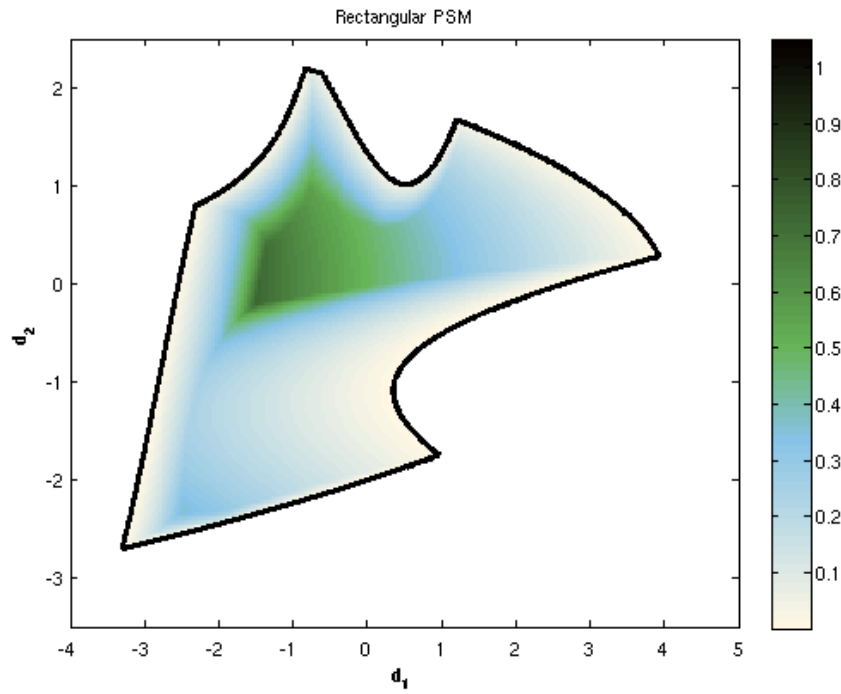
American Institute of Aeronautics and Astronautics

Figure 4. Rectangular PSMs for $\mathcal{R}(\bar{p}, m1)$.
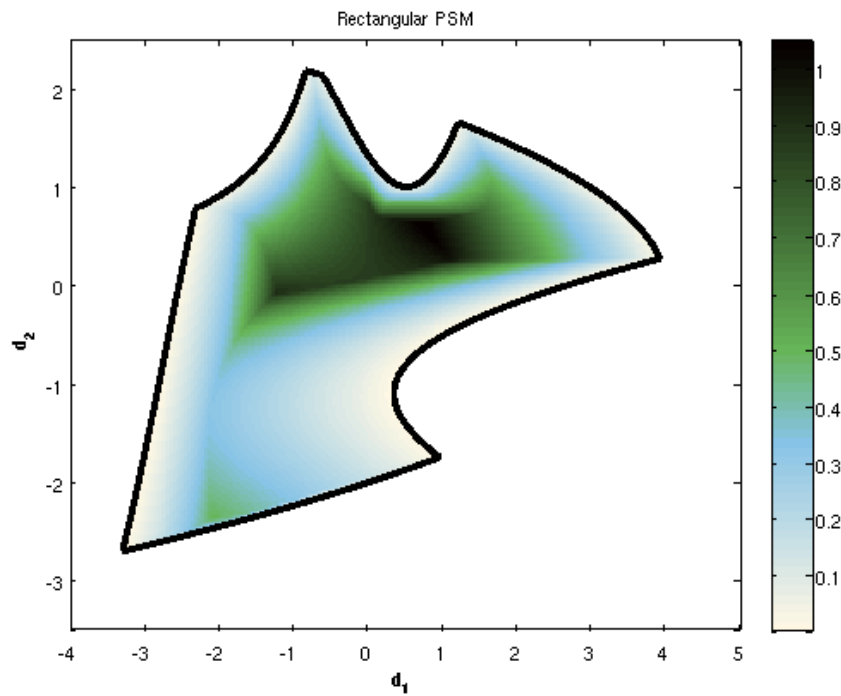
Figure 5. Rectangular PSMs for $\mathcal{R}(\bar{p}, m2)$.

American Institute of Aeronautics and Astronautics

sider the triangular support set shown in the left of Figure 6 with a solid line. The tightest bounding circle and rectangle are superimposed. Clearly, the rectangle better approximates the triangular set. The Robust Design Spaces corresponding to both bounding sets, calculated via spherical-PSMs and rectangular-PSMs, are shown in the right subplot of Figure 6. The Robust Design Space for the bounding circle is filled in with black while the Robust Design Space for the bounding rectangle is colored in dark gray. As expected, the Robust Design Space for the rectangle contains the one for the sphere. We have no such tools for the determination of the true Robust Design Space for the triangular support set, so we apply an approximation technique. For this, a probability density function having the triangle as the support set is assumed. In a probabilistic model, the Robust Design Space is given by $\{\boldsymbol{d} : P[\mathcal{F}] = 0\}$. The approximation technique results from estimating the equality in this expression using sampling. In theory, this approximation depends on the support set only, not on the probability density function assumed. In practice, this is not the case due to the numerical error caused by using a sample set of finite size. The corresponding Robust Design Space approximation is colored with light gray in Figure 6. The bounding-based approximations are both subsets of the sampling based approximation. The conservatism introduced by using the bounding circle leads to a considerably smaller Robust Design Space approximation. Note that the portion of the Robust Design Space in the vicinity of $\boldsymbol{d} = [-2, -2.25]^T$ is completely omitted by this approximation. Evidently, the Robust Design Space corresponding to the rectangle is a better approximation since the offset between the rectangle and the triangle is smaller. This conservatism introduced by bounding might lead to an empty approximation of the Robust Design Space, even though the actual Robust Design Space is non-empty. Notice however, that while sampling-based Robust Design Space approximation is the largest, only the approximations resulting from the bounding sets are verifiable. This is so, since when the support set is a hyper-sphere or a hyper-rectangle, the actual Robust Design Space, providing it is not empty, can be calculated exactly.

The tools of Section V for robust-design are used next. While the search for the design with best robustness characteristics corresponding to a circular support leads to $\boldsymbol{d}^{\mathcal{S}} = [-1.65, -0.33]^T$ and $\mathcal{M} = \mathcal{S}_{\boldsymbol{p}}(\bar{\boldsymbol{p}}, 0.53)$, the one corresponding to the rectangular support set $\mathcal{R}_{\boldsymbol{p}}(\bar{\boldsymbol{p}}, \boldsymbol{m2})$ leads to $\boldsymbol{d}^{\mathcal{R}} = [0.718, 0.631]^T$ and $\mathcal{M} = \mathcal{R}_{\boldsymbol{p}}(\bar{\boldsymbol{p}}, 0.26\boldsymbol{m2})$. These sets are shown in Figures 7 and 8 along with the corresponding Critical Parameter Values. Note that changing the design point has altered the constraint boundaries. Three Critical Parameter Values exist in both cases. Recall that support sets proportional and larger than $\mathcal{M}$ lead to an empty Robust Design Space.
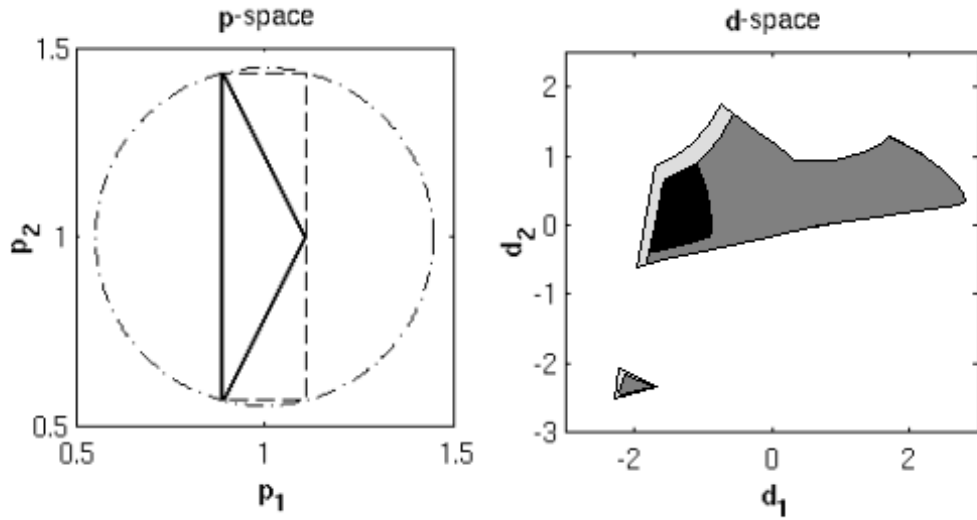
Figure 6. Left: triangular support set and outer bounding sets. Right: corresponding Robust Design Space approximations.
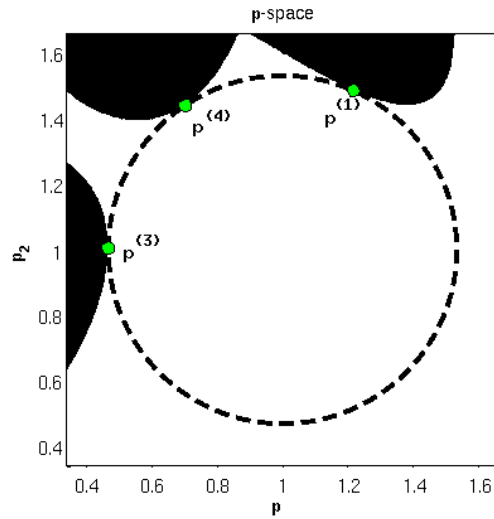

Figure 7. Maximum feasible set

B. Flutter Speed Analysis

In this example we study the flutter speed of the simple aeroelastic model shown in Figure 9. Reference[17] provides supporting information. While the aerodynamic forces and moments are applied at the quarter chord point of the wing, the location of the center of gravity of the system can be adjusted by changing the distance d between the movable mass m_2 and
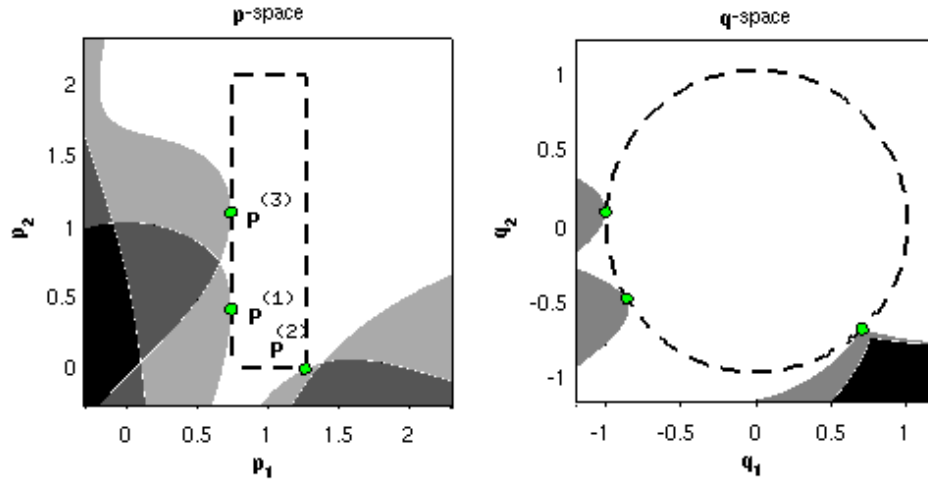
American Institute of Aeronautics and Astronautics

Figure 8. Left: maximum feasible set proportional to $\mathcal{R}(\bar{p}, m2)$. Right: corresponding set in q-space.
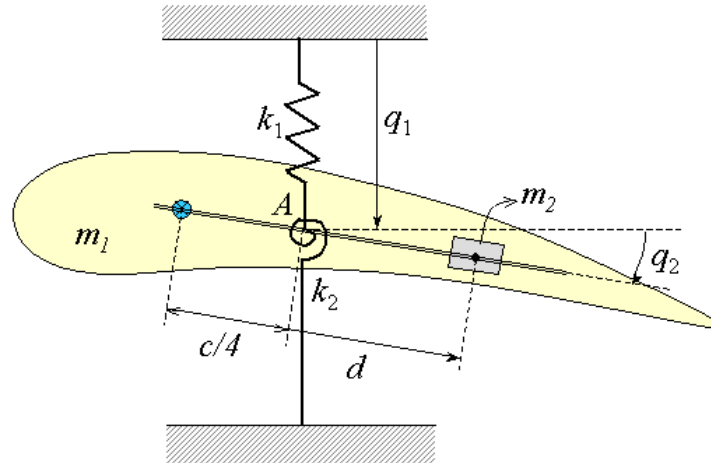

Figure 9. Two degrees of freedom flutter model

the elastic axis A. The linearized equations of motion are given by

$$
\begin{bmatrix} \dot{x} \\ \ddot{x} \end{bmatrix} = \begin{bmatrix} \mathbf{0} & \mathbf{I} \\ -\mathbf{M}^{-1}\mathbf{K} & -\mathbf{M}^{-1}\mathbf{C} \end{bmatrix} \begin{bmatrix} x \\ \dot{x} \end{bmatrix},
\tag{22}
$$

American Institute of Aeronautics and Astronautics

where $\boldsymbol{x} = [q_1, q_2]^T$ is the state space vector and

$$\mathbf{M} = \begin{bmatrix} m_1 + m_2 & m_1 l + m_2 d \\ m_1 l + m_2 d & I_A + m_2 d^2 \end{bmatrix}, \quad \mathbf{C} = qs \begin{bmatrix} C_{l\alpha}/4 & 0 \\ -cC_{l\alpha}/(4u) & -cC_{m\alpha} \end{bmatrix},$$

$$\mathbf{K} = \begin{bmatrix} k_1 & qsC_{l\alpha} \\ 0 & k_2 - qscC_{l\alpha}/4 \end{bmatrix}.$$

In these expressions, m_1 is the mass of the wing, l is the distance between A and the center of gravity of the wing, c is the cord length, s is the wing's reference area, I_A is the moment of inertia of the wing about A, q is the dynamic pressure, u is the free stream velocity, $C_{l\alpha}$ and $C_{m\alpha}$ are stability derivatives, and k_1 and k_2 are the bending and torsional stiffnesses respectively. For simplicity sake we have assumed that d varies slowly enough to neglect the Coriolis effect.
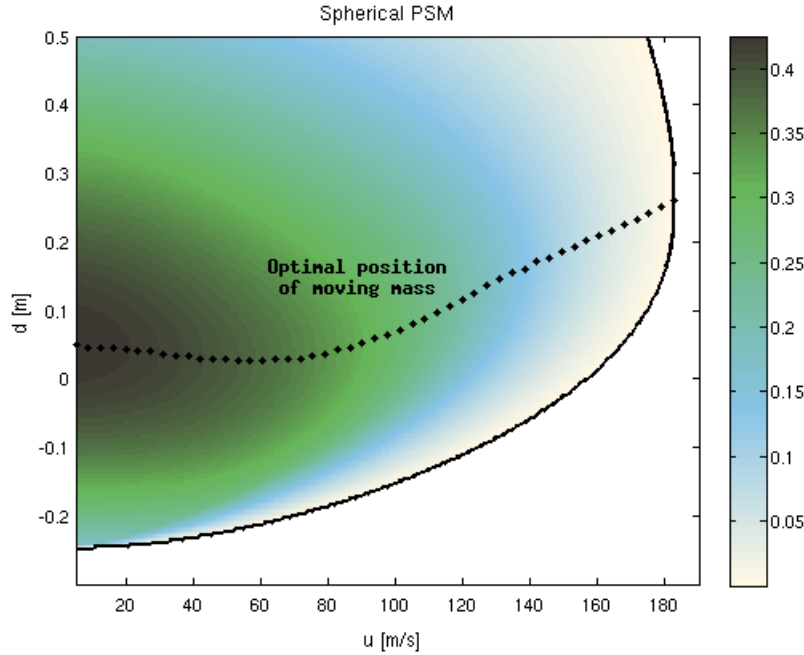
Figure 10. Spherical-PSMs in the nominally stable $\langle u, d \rangle$ space

The following numerical values are assumed: $m_1 = 0.5~kg$, $m_2 = 0.5~kg$, $l = 0.1~m$, $I_A = 0.1~kgm^2$, $q = 0.6125u^2~kg/m^3$, $s = 1~m^2$, and $c = 1~m$. The parameters $C_{l\alpha}$, $C_{m\alpha}$, k_1 and k_2 are considered uncertain. A non-dimensional $\boldsymbol{p}$-space is obtained by using the

American Institute of Aeronautics and Astronautics

parametrization

$$[C_{l\alpha}, C_{m\alpha}, k_1, k_2]^T = \text{diag}\{[2\pi, 0, 6 \times 10^5, 10^5]\}\boldsymbol{p} + \text{diag}\{[0, 0.01, 0, 0]\}(\boldsymbol{p} - \bar{\boldsymbol{p}}),$$

where $\bar{\boldsymbol{p}} = [1, 1, 1, 1]^T$. Design requirements for flutter speed are given by the set of constraints $\boldsymbol{g}_i = Re\{\lambda^{(i)}\}/\|\lambda^{(i)}\|$ for $i = 1, \dots, 4$; where $\lambda^{(i)}$ is the i-th eigenvalue of the matrix in Equation (22).

In this example, the Feasible Design Space is given by the $\langle u, d \rangle$ pairs for which the system is stable when $\boldsymbol{p} = \bar{\boldsymbol{p}}$. The distribution of spherical-PSMs in the Feasible Design Space is shown in Figure 10. The position of the moving mass that maximizes the spherical-PSM at each particular u is superimposed.
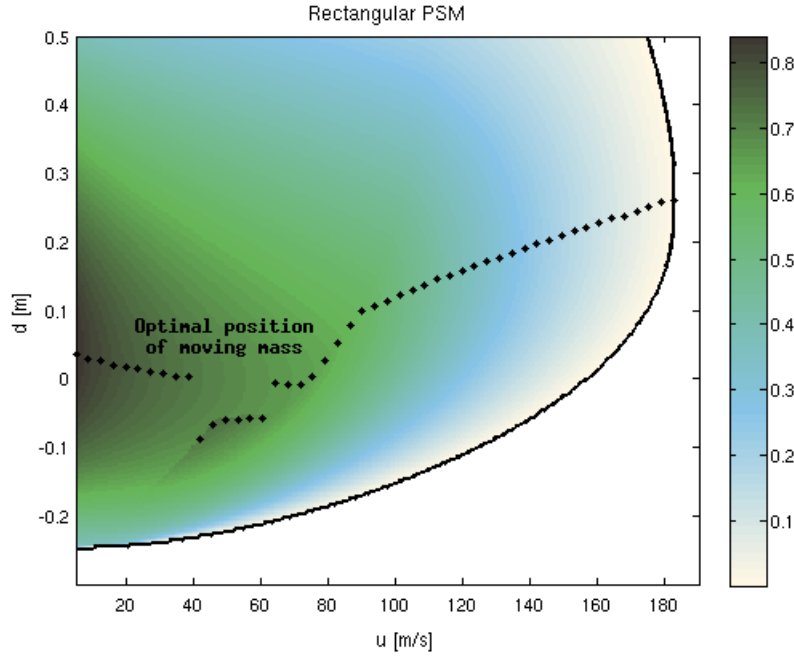

Figure 11. Rectangular-PSMs in the nominally stable $\langle u, d \rangle$ space

Expansions of the hyper-rectangle centered at $\bar{\boldsymbol{p}}$ with $\boldsymbol{m} = [20, 4, 5, 10]$ lead to Figure (11). As before, the most robust positions of the moving mass are superimposed. Note that the local maximum near $\langle u, d \rangle = \langle 48, -0.06 \rangle$ makes the resulting trail discontinuous. Note also that in the vicinity of this maximum the rectangular-PSM function $\rho_{\mathcal{R}}(u, d)$ is also discontinuous. This phenomenon implies that a differential change in u or d produces a sizable, non-small change in $\mathcal{F}$, hence on the corresponding PSM. Sudden changes like this one denote the occurrence of a bifurcation. The comparison of Figures (10) and (11) indicates the sensitivity of the robustness metrics to the geometry of the uncertainty model.

American Institute of Aeronautics and Astronautics

VII. Concluding Remarks

A methodology for robustness analysis and robust-design of systems subject to parametric uncertainty has been proposed. Emphasis was given to uncertainty sets prescribed or bounded by hyper-spheres or hyper-rectangles. The tools developed herein enable the exploration of the targeted regions of the design space where the design requirements are satisfied for all parameter values in the uncertainty set. Formal assessments of robustness are possible since these sets lend themselves to a rigorous mathematical treatment for which sampling/partitioning the parameter is not required. Extensions that enable the efficient search for designs with improved robustness characteristics have also been proposed. By sizing the maximum uncertainty set for which the design requirements are still satisfied, we can determine the transition point at which hard constraints can no longer be enforced. A comparison of any given uncertainty model, deterministic or probabilistic, with the maximum set enable us to determine which numerical methods must be used. This is of paramount importance since numerical tools typically used in reliability-based design optimization, such as sampling and the first order reliability method, are inapplicable, ineffective, or inconclusive when dealing with hard constraints. The scope of the ideas proposed is generic, making them applicable to a broad spectrum of engineering problems.

References

[1]Kall, P. and Wallace, S., *Stochastic Programming*, Wiley, New York, 1994.

[2]Ermoliev, Y., "Stochastic quasigradient methods and their applications to systems optimization," *Stochastics*, Vol. 9, No. 1, 1983, pp. 1–36.

[3]Rackwitz, R., "Reliability analysis, a review and some perspectives," *Structural Safety*, Vol. 23, 2001, pp. 365–395.

[4]Luis, R. M., Teixeira, A. P., and Soares, C. G., "Longitudinal strength reliability of a tanker accidentally grounded," *European Sefety and Reliability Conference*, Estoril, Portugal, September 18-22 2006, Vol 2, 1499-1509.

[5]Crespo, L. G. and Kenny, S. P., "Reliability-based control design for uncertain systems," *AIAA Journal of Guidance, Control, and Dynamics*, Vol. 28, No. 4, 2005.

[6]Darligton, J., Pantelides, C., Rustem, B., and Tanyi, B., "An algorithm for constrained nonlinear optimization under uncertainty," *Automatica*, Vol. 35, 1999, pp. 217–228.

[7]Mulvey, J. N., Vanderbrei, R. J., and Zenios, S. A., "Robust optimization of large scale systems," *Operations Research*, Vol. 2, No. 43, 1995, pp. 264–280.

[8]Gustafson, S. A., *Semi-infinite programming and applications*, Springer, Berlin, 1981.

[9]Howe, M. A., Rustem, B., and Selby, M. J. P., "Multi-period minimax hedging strategies," *European Journal of Operations Research*, Vol. 1, No. 93, 1996, pp. 185–204.

[10]Rustem, B. and Nguyen, Q., "An algorithm for the inequality constrained minimax problem," *SIAM Journal of Optimization*, Vol. 8, No. 1, 1998, pp. 265–283.

American Institute of Aeronautics and Astronautics

[11]Tenne, D. and Singh, T., "Efficient Minimax Control Design for Prescribed Parameter Uncertainty," *AIAA Journal of Guidance, Control and Dynamics*, Vol. 27, No. 6, 2004, pp. 1009–1016.

[12]Engelund, S. and Rackwitz, R., "A benchmark study of Importance Sampling techniques in structural reliability," *Structural Safety*, Vol. 12, No. 4, 1993, pp. 255–276.

[13]Mahadevan, S. and Raghothamachar, P., "Adaptive simulation for system reliability analysis of large structures," *Computers and Structures*, Vol. 77, No. 6, 2000, pp. 725–734.

[14]Robinson, D. and Atcitty, C., "Comparison of quasi- and pseudo- Monte Carlo sampling for reliability and uncertainty analysis," *AIAA Structures, Structural Dynamics and Materials Conference*, Vol. 1, AIAA 1999-1589, pp. 2942–2949.

[15]Royset, J., Kiureghian, A. D., and Polak, E., "Reliability-based optimal structural design by the decoupling approach," *Reliability Engineering and System Safety*, Vol. 73, 2001, pp. 213–221.

[16]Crespo, L. G., Giesy, D. P., and Kenny, S. P., "Strict Feasibility in Optimization under Uncertainty," *11th AIAA/ISSMO Multidisciplinary Analysis and Optimization Conference*, Portsmouth, VA USA, September 2006, AIAA-2006-7035.

[17]Bisplinghoff, R. L. and Halfman, R. L., *Aeroelasticity*, Addison-Wesley, New York, 1955.

American Institute of Aeronautics and Astronautics